Assessment Cover

Module No:	**ENGR7015**	Module title:	**Advanced Vehicle Dynamics**

Assessment title:	**Portfolio Coursework**

Due date and time**:**	13:00hrs Friday 23rd December 2022.

Estimated total time to be spent on assignment:	**80 hours per student**

LEARNING OUTCOMES

On successful completion of this module, students will be able to achieve the module following learning outcomes (LOs): *LO numbers and text copied and pasted from the module descriptor*.
LO 1: Demonstrate a systematic and ordered understanding of vehicle performance backed up with analytical determination of performance;
LO 2: Perform complex analyses on whole vehicle performance and critically assess one vehicle against another.
LO 3: Critically examine current methods of vehicle performance evaluation
LO 4: Use numerical and analytical techniques to critically analyse different aspects of vehicle performance.
LO 5: Make rational and informed decisions to select methods for improving vehicle performance over a wide range of situations.
LO 7: Undertake independent learning of 'new vehicle dynamics related problems' at an advanced level

Engineering Council AHEP4 LOs assessed (from S1 2022-23):	
M1	Apply a comprehensive knowledge of mathematics, statistics, natural science and engineering principles to the solution of complex problems. Much of the knowledge will be at the forefront of the particular subject of study and informed by a critical awareness of new developments and the wider context of engineering
M2	Formulate and analyse complex problems to reach substantiated conclusions. This will involve evaluating available data using first principles of mathematics, statistics,

	natural science and engineering principles, and using engineering judgment to work with information that may be uncertain or incomplete, discussing the limitations of the techniques employed
M3	Select and apply appropriate computational and analytical techniques to model complex problems, discussing the limitations of the techniques employed
M4	Select and critically evaluate technical literature and other sources of information to solve complex problems
M17	Communicate effectively on complex engineering matters with technical and non-technical audiences, evaluating the effectiveness of the methods used

STUDENT NAME(S)

Student No:	Student Name:	Group Name and Number:
1.	**PLEASE DO NOT ADD YOUR NAME AS SUBMISSION AND ASSESSMENT IS ANONYMOUS**	

Statement of Compliance *(please tick to sign)*

x	I declare that the work submitted is my own and that the work I submit is fully in accordance with the University regulations regarding assessments (*www.brookes.ac.uk/uniregulations/current*)

CONTENTS

1 TYRE MODELS

Tire models are representations that reproduce the behaviour of tires in the real world. They are approximations, and therefore they are subject to errors, which opens the door to many different approaches, with their advantages and disadvantages. Consequently, it is a topic that has never been fully developed, hence the amount of different approximations that people have come up with. In this work, three of these tyre models are presented: Gipser's FTire, Shabana's ANCF Tire, and Gallrein's CD Tire.

1.1 FTIRE

The Flexible Ring Tire Model is a non-linear vibration model that represents the tire as a flexible ring belt that is able to displace and bend in definite directions in relation to the rim. This also includes lateral displacement. It was born as a solution response to very time-consuming models, and pure in-plane models that cannot be used simultaneously for comfort and handling investigations. Thus, it works for both comfort and handling studies.

Modelization

The tire belt is described as a numerically defined number of point masses, each of coupled with their direct neighbours by stiff springs and bending stiffnesses in-plane and out-of-plane. All the point masses are assembled in an extensible and flexible belt, which has stiffness in the radial, tangential and lateral directions with respect to the rim.

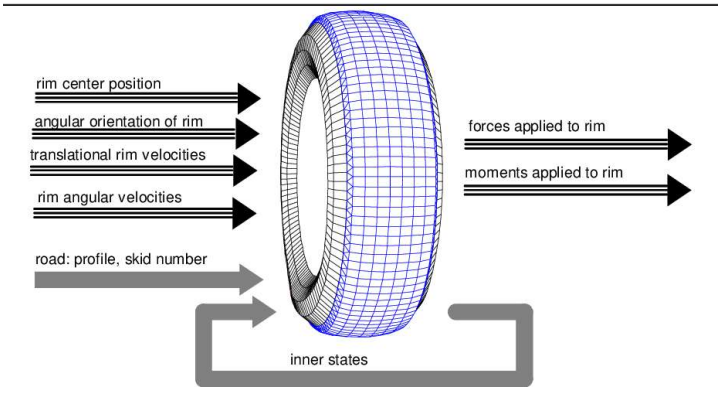

Figure 1. FTire mesh model

All the stiffnesses are defined in the pre-processing, depending on the modal parameters.

Attached to every point mass or element there are a number of predefined mass-less tread ribs. They carry nonlinear stiffness and damping properties in the radial direction, which depend on road profile, locus, and orientation of the associated belt elements; and the tangential and lateral directions, which are determined by the sliding velocity on the ground and the local values of the sliding coefficient. This sliding coefficient depends on the ground pressure and sliding velocity relatively to the rib end point velocity projected onto the road profile tangent plane. Certain precautions have been undertaken not to let the ground pressure distribution mirror the polygonal shape of the 'belt chain'.

By integrating the forces in the elastic foundation of the belt, we can obtain all six forces in the tire.

The model has very little restrictions in terms of longitudinal, lateral and vertical vehicle dynamic situations; but it serves as an accurate simulation up to relatively high frequencies. No additional computing effort is needed for a complete stand still.

The main employability of FTire is exclusively for computer simulation processes and especially, implementation to Adams software.

In terms of the input needed, it involves normal measurements of the tire to be simulated, such as rolling circumference, rim diameter, width of tread, and tire mass; as well as some other more specific parameters such as natural frequencies of first, second, fourth, fifth and sixth mode.

Among the CPU performance, it purely depends on the number of elements used to represent the tire, which increases proportionally. It also depends proportionally on the time scale used between iterations.

Finally, the sample results suggest very accurate results, but slightly underestimated. However, the amount of time saving and optimization that this model presents in comparison with other more computer demanding models is very notable, especially for the very extreme and more CPU expensive cases.

1.2 ANCF TIRE

For hybrid ANCF models that consist of a rigid and a flexible body with intersections, the main problems that hinder their development is the treatment of constraints at the boundaries between the two bodies. To solve this, the ANCF-RN is defined as Absolute Nodal Coordinate Formulation Reference Node, which offers the possibility to develop new and complex multibody system models. It is not associated with any finite element, but the location is established by constraints and joints using linear algebraic equations, which are related to the coordinates of other nodes.

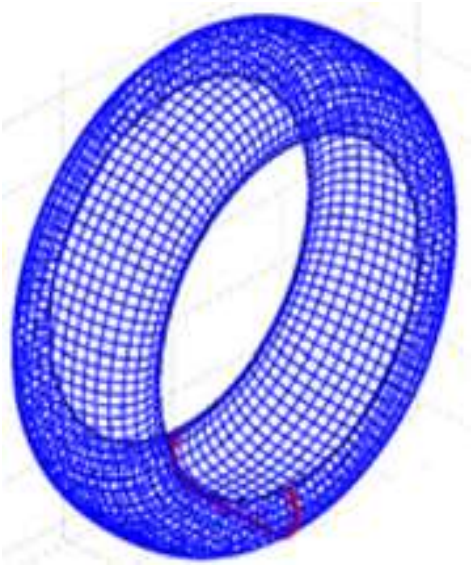

Figure 2. ANCF Tire mesh model

This concept can be used to model tire assemblies, among other things, using a mesh developed by ANCF finite elements, which allows for arbitrarily large displacements in rotation and deformation. There are assumptions made on this model that define the rigidity of the mesh reference. It also includes physics continua allowing for pressure calculations in both the inside and outside of the tire.

1.3 CD TIRE

CD Tire defines itself as a scalable tire model for full vehicle simulations that is able to interact with 3D road surfaces and accurately capture the vibrations behaviour. It has different physical models for the belt, sidewall and treat to ensure accuracy and performance for different applications, such as ride comfort, harshness analysis, durability analysis and handling analysis, among many others.

CD Tire is available in MATLAB and ADAMs, and has a wide variation of models suitable for different studies and computational requirements. CD Tire is composed of a family of 3 different models, each one more advanced, and base themselves on the ring and brush models, implementing them into a whole system. It is defined as a microscopical physical description, with the aim to reduce the calculation speed required by other finite-element-based models.

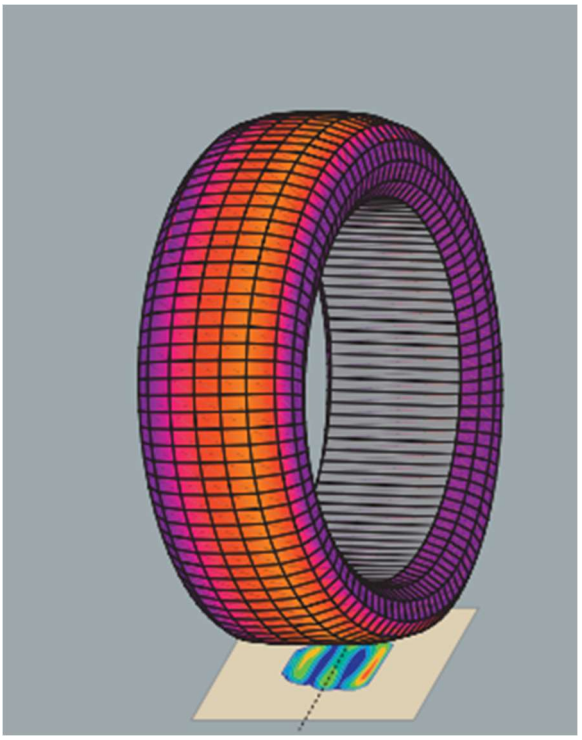

Figure 3. CD Tire Mesh model

1.4 DISCUSSION

Taking a closer look at the three different models, it is very clear that they serve different purposes by themselves. While FTire focus itself on a fast, approachable calculation to be implemented and run in accessible computers and programs such as MATLAB, ANCF Tire looks for precision while even implementing a physics continua to get pressure distributions along the tyre surface. Meanwhile CD Tire, as being a much more recent model, implements different technologies to an approachable scheme with the objective to become a new industry standard.

In conclusion, it can be said that FTire is a model on the decline as new better models are developed while maintaining the computational performance of it, such as CD Tire. A comparison between which model to use in each scenario is described below.

Analysis Precision	**Computer Power Available**		
	Low	*Medium*	*High*
Fast	Ftire	Ftire, CD Tire	CD Tire
Medium	Ftire , CD Tire	CD Tire	ANCF Tire, CD Tire
Precise	CD Tire	ANCF Tire	ANCF Tire

Table 1. Tire Model Comparisons and selectivity by different requirements

2 BICYCLE MODEL ANALYSIS

2.1 PARAMETERS

Mass	900 kg
Polar moment Izz	1100 kg.m2
CoG to front axle distance	0.9 m
Wheelbase	2.6 m
Front cornering stiffness	1100 N/deg
Rear cornering stiffness	900 N/deg
Steer input	10 degrees
Velocity	35m/s

Table 2. Vehicle data for bicycle model

2.2 MODEL AND NUMERICAL CALCULATIONS

A comparison of the bicycle model dynamics was made between a derivative analysis using MATLAB and the dynamic model in Adams, for vehicle and conditions underlined in Table 2. The yaw velocities were plotted to analyse the performance of both methods. In this case, a step steer input of 10 degrees was applied at 2.5 seconds from the start of the simulation. The MATLAB values were offset to match the Adams ones.

In this first case, we can see how the MATLAB results are slightly underestimated in comparison to Adams, under figure 4.

Using the basic equation of cornering:

$$\delta = \frac{l}{R} + Ka_Y \qquad eq.1$$

And applying the neutral steering vehicle assumption where $\delta = \frac{l}{R}$, we can achieve the neutral steering condition of the vehicle accounting for the understeering gradient (K) being equal to 0. This can be achieved by changing the parameters of our vehicle, specifically, cornering stiffness of the tyres (which is equivalent to changing the tyre properties) or changing the location of the centre of gravity.

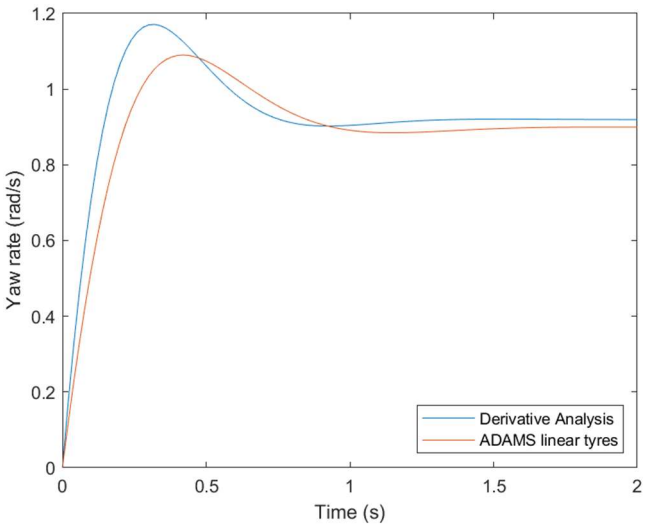

*Figure SEQ Figure * ARABIC 4. Yaw rate comparison between derivative analysis and ADAMS for a transient steer input of 10 degrees.*

According to the derivative analysis, assuming the critical velocity is sufficiently high and the understeering gradient tends to 0, the neutral steering vehicle condition can be achieved by:

- Moving the centre of gravity to 45% of the wheelbase from the front, while keeping the rest of the parameters intact (Blue line).
- Changing the front cornering stiffness to 1700 deg/N, while keeping the rest of the parameters intact (Yellow line).
- Changing the rear cornering stiffness to 582 deg/N, while keeping the rest of the parameters intact (Orange line).

In all three scenarios, the yaw rate is linearly dependent on the velocity speed, as seen in Figure 5.

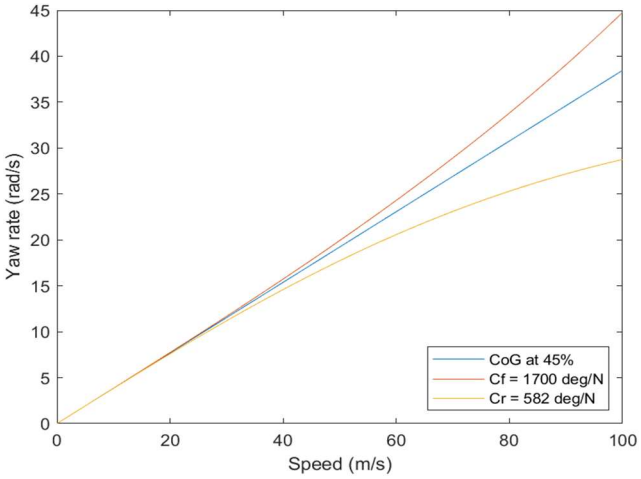

Figure 5. Yaw rate comparison for 3 different methods of achieving the neutral steering vehicle.

From the basic equation of cornering:

$$\delta = \frac{l}{R} + \alpha_F - \alpha_R \qquad eq.\ 2$$

The neutral steering condition is achieved when $\alpha_F - \alpha_R = 0$, once the turn is stabilised. Using Adams, this condition is met when a = 1.420 metres.

A further development was introduced by using non-linear tyre models into the Adams simulation. This creates a maximum force which can be achieved at 6 degrees of steering input, from which the tyre starts to “slip” and therefore, cannot create additional force as the slip angle increases. This is represented in Figure 6, and compared to the linear behaviour at very low slip angles.

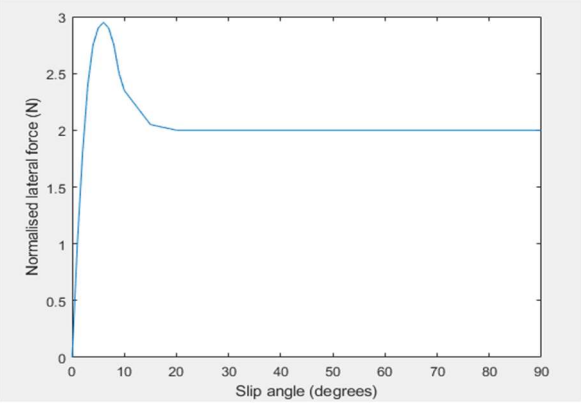

Figure 6. Non-linear tyre modification to lateral force as a function of slip angle

We can see that the maximum is achieved at 6 degrees of slip angle, and that the similarity between both behaviours is only achieved at 1 degree of slip angle.

This reduction in the lateral force is manifested in the yaw velocity as we increase the steer input. Even at a steer input of 1 degree, shown in Figure 7, a reduction of the yaw velocity is already appreciable, which is caused by the higher slip angle of the front tire due to the vehicle tendency to oversteer.

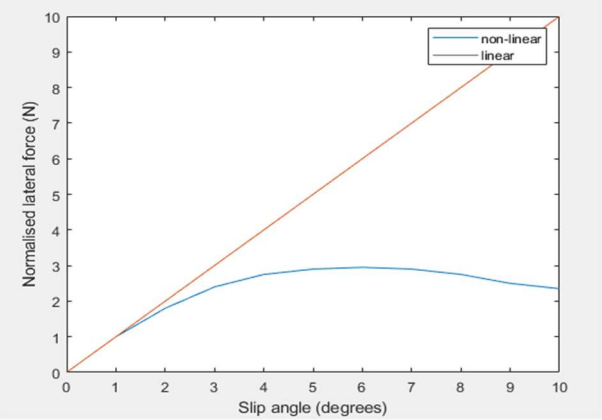

Figure 7. Normalized lateral force for different slip angles at a linear and non-linear stage

This indicates that the linear tyres bicycle model is only valid for small angles of steer, hence the small angle approximation carried out to obtain the derivatives analysis.

At 10% of the determined speed (35 m/s) the slip angle is reduced, bringing the model to a close-to-linear behaviour. However, taking a look at Figure 8, which shows the comparison between the stable yaw rate at different speeds at a linear and non-linear configuration, for a 1-degree steering input, there is still a loss in yaw rate.

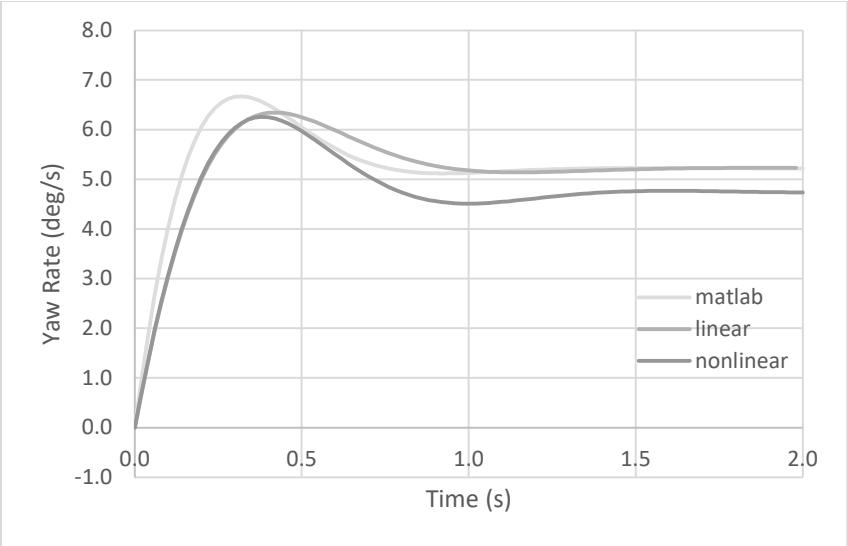

Figure 8. Yaw rate comparison for a transient steer input of 1 degree at a linear, non-linear and derivative analysis state

It was also found that the slip angle achieved by the tires is also dependent on the speed at which the turn is applied.

$$V_{crit} = \sqrt{-\frac{1}{K}} \qquad eq.\ 3$$

Where K is the understeer gradient, which is -1.85 for this vehicle.

The two lines start to differ at the critical speed of 5.56 m/s, using equation 3. Past this point, the linear region of the tires is surpassed, and the vehicle acquires an underdamped steering response, as shown in Figure 9.

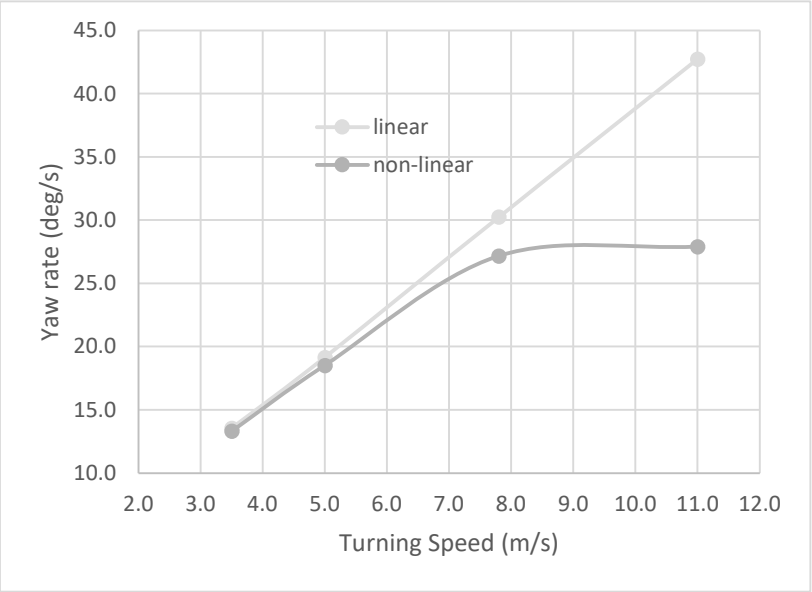

Figure 9. Adams' obtained stabilised yaw rate for linear and non-linear states as a function of turning speed.

`

2.3 FURTHER DEVELOPMENTS

A series of future developments for the model can be considered in order to make it more robust regarding other different steering situations.

First of all, the main limitation of this bicycle model relies on the fact that it only has two wheels. Left and right slip angles are not exactly the same as this model assumes, but are rather related to each side's path to the cornering centre. This might introduce a concept by the name of Ackerman Steering, which suggests that the inside front tyre must steer at a larger angle than the outside, in order to avoid sliding. (Vogel, n.d.)

Furthermore, this model also completely ignores vertical vehicle dynamics, which means there is no consideration of vertical aerodynamic loads, roll steering, or even weight transfers.

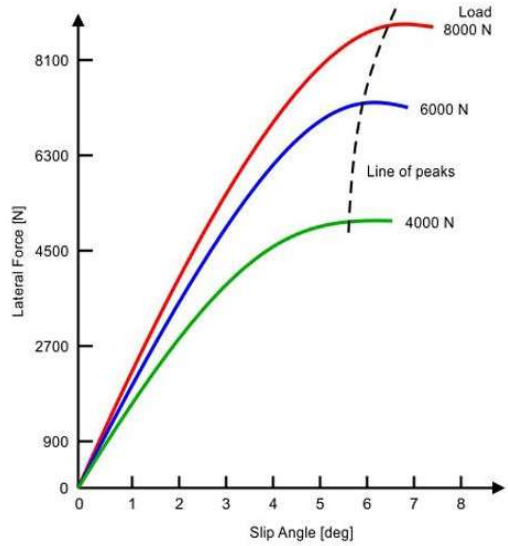

Figure 10. Lateral Force variation at different vertical loads on the wheels

As seen in Figure 10, the maximum lateral force of the tyre is dependent on the vertical load acting on it, which restricts the slipping region making the tyre sturdier to higher slip angles (Suspension Secrets, n.d.). This also works inversely, as the tyre load is decreased, so does the maximum force available from it. In a 4-wheel vehicle turning scenario, external vertical loads acting on it such as the aerodynamic downforce will increase the turning performance of the vehicle at higher speeds.

This same vertical load variation can be applied to the vehicle rolling moments. When steering input is applied, there is some weight displacement which increases the load on the outside tyres, while reducing the load on the inside ones. However, this is not a linear trade-off, as seen in Figure 10, and there are lateral force losses in this phenomenon. As a comparison, our model described above assumes a 50% load distribution at all times, which is not exactly what happens in reality.

In addition to this, the concept of roll steering results in small changes in the slip angle of the tyres when they are moved up or down, as a consequence of the suspension geometry and behaviour during cornering, modifying the steering of the pair of wheels in the same axle when the body rolls (Dixon, 1996). This will have an obvious effect on the steering dynamics of the model, introducing a now roll steer coefficient, which modifies the steering angle, and therefore also modifies the steering dynamics of the car by inducing over or understeer and a modified response of the driver to overcome this, known as roll understeer angle.

In terms of longitudinal dynamics, the concept of weight transfer is also applicable, but only in a non-stable condition of braking or accelerating. The steering response of the vehicle due to changes in acceleration is known as Power steer, which is very closely related to the differentials of the vehicle itself. This has an additional effect on the weight distribution, and the tyre load between front and rear, just in the same way as with the roll characteristics described above. As the vehicle breaks, the deceleration will shift the weight towards the front, loading the front tyres and therefore increasing their lateral performance ever so slightly.

Vehicle roll dynamics can be implemented as a explicit variable that introduces roll angle and roll angular speed in the 3 degree of freedom model described by Dixon (Dixon, 1997), which introduces a 3rd motion equation that takes into consideration the roll, along with 5 more new derivatives to the ones investigated in the simple bicycle model: Y_{ϕ}, N_{ϕ}, and L_p, L_{δ}, and L_{ϕ}, where L denotes the rolling moment.

There are many other effects worth mentioning that also can alter the cornering behaviour or the vehicle, for example, banking, compliance steering, ride height or even wind forces.

3 SUSPENSION OPTIMIZATION

For the suspension optimization, the Lancia 037 Rally Spec data will be used as a reference, tabulated in table 3. The suspension will be optimised for different degrees of freedom models, comparing the results obtained.

3.1 DATA

Mass	960 kg
Length	3.92 m
Wheelbase	2.45 m
Weight distribution	42% front / 58% rear

Table 3. Lancia 037 Rally spec data for suspension optimization

Two types of input were analysed, the pothole and the road profile. Spring force and the body acceleration were taken as measurements, simulating the contact patch force and the chassis upwards acceleration; minimising the first one would improve grip and performance as the tyre load variation is reduced, whilst minimising the second one would improve comfort. For our vehicle, we are interested in performance, and therefore contact patch force.

3.2 1 DEGREE OF FREEDOM

A 1 degree of freedom model was presented for optimization. For this particular case, the higher the spring stiffness, the higher the spring force generated on the tyre. Therefore, an arbitrary value of 100N/mm was set. This accounts for a quarter of the car. In this case, a whole car is bound to be measured, and following equation 4, for parallel springs:

$$k_{res} = k_1 + k_2 + \cdots k_n \qquad \textit{eq. 4}$$

Accounting for 4 wheels and a total weight of 960kg, the stiffness is set to 400N/mm.

The pot hole simulation was set to be a curb of 10mm upwards. A value for the ideal damping was found to be 0.43 for the lowest contact patch force variation, which is set to be 16.85 newton-sec/mm.

For the exponential sine sweep input, a value of 0.293 was found for a sweep of amplitude 10mm. This is translated to 11.36 newton-sec/mm. It was found that for each input, there was no difference between the normalised values of the contact patch force and body acceleration, which means a limitation in such a 1 degree of freedom model. Furthermore, we are ignoring the tyre effects. This sort of model would

be more suitable for no-tyre environments or tyres that can be considered rigid, such as trains.

3.3 2 DEGREES OF FREEDOM

For the 2 degrees of freedom system, the same procedure was followed as the 1DoF. In this case, accounting for equation 1, a 4-tyre representation is introduced as mass of 360kg and an undamped spring with a stiffness of 600 N/mm (close to a wheel performance), and again, the damped spring was fixed to a value of 400N/mm.

The sweep input was set to 5mm of maximum amplitude.

As our vehicle is meant for performance, our biggest factor is the tyre force variation. Using a cost function, a trade-off function is created that optimises the damping coefficient. In this case, we have chosen weights of 0.7 for the CPL and 0.3 for the chassis acceleration.

Table 4 shows the result for different inputs and optimisation factors. The optimum damping value is different depending on the input. Since the sweep input also covers a higher range of possible interactions for the suspension, it has been used as a primary input for the Cost Function. It was found that the best optimal damping value is 0.53, equivalent to 20.77 newton-sec/mm. Furthermore, it is very clear that the optimal values for all 5 curves are established around the 0.5-0.55 area. In this model, the only present movement is heave, meaning no pitch of any sort is modelled. A comparison graph of the normalised measures for different scenarios is seen in Figure 11.

Optimisation and Input	***Optimal Damping ratios***	***Equivalent Damping Coefficients (newton-sec/mm)***
CPL (pothole)	0.47	18.42
CPL (sweep)	0.47	18.42
Acceleration (pothole)	0.52	20.38
Acceleration (sweep)	0.62	24.30
Optimised Cost Function (sweep)	0.53	20.77

Table 4. Results for optimal Damping ratios and coefficients for different input scenarios and measures

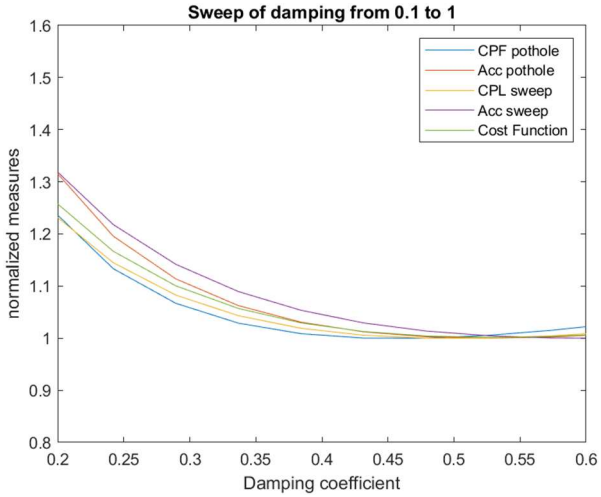

Figure 11. Normalised measures for different input scenarios as a function of a selected range of damping ratios

3.3.1 Non-linear 2 degrees of freedom

The models described above consider spring dampers to behave linearly. This is not true for most vehicle manufacturers, and therefore it must be possible to optimise the bound and rebound parameters of spring dampers. A non-linear model of the previous model was presented with the objective to optimise said parameters.

Following equation 5, where:

$$F_{damping} = -v * c_{bound,rebound} \qquad \text{eq. 5}$$

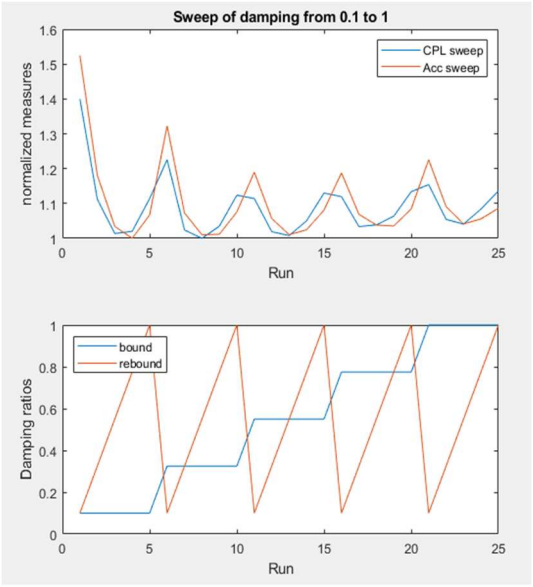

Figure 12. normalized measures at each run and their respective damping ratio values for bound and rebound

As the coefficient changes from bound to rebound conditions, the force will also change, and any chance to further optimise the suspension can be exploited.

For this case, a sweep of damping coefficients between 0.1 and 1 was made for both bound and rebound parameters, using the sweep input. It was found, as seen in Figure 12, that the best values for contact patch force and body vertical acceleration are found at different runs, meaning we have to consider what performance factor we are more interested in. A more refined optimization was made using smaller intervals from the results obtained. A cost function was also employed to find the best balance for the desired performance as described in the previous model. The optimal results are presented in Table 5.

Optimisation Parameters	*Optimal damping ratios*		*Equivalent Damping Coefficients (newton-sec/mm)*	
	Bound	*Rebound*	*Bound*	*Rebound*
Body acceleration	0.10	0.70	3.92	27.43
Contact Patch force	0.25	0.60	9.80	23.52
Cost Function	0.21	0.61	8.23	23.91

Table 5. Results for optimal damping ratios for the different optimisation parameters and their respective damping coefficients.

3.3.2 Linear 4 degrees of freedom

For this case, the same vehicle parameters were used as above. The model represents a side view as a half vehicle model, subject to heave and pitch moment rotation. Both front and rear springs and wheel masses represent the theoretical springs of both left and right sides of the car. The sweep input was used with a slight offset of 0.1 seconds between the front and the rear, which introduces a velocity dependency on the response of the vehicle for such a speed.

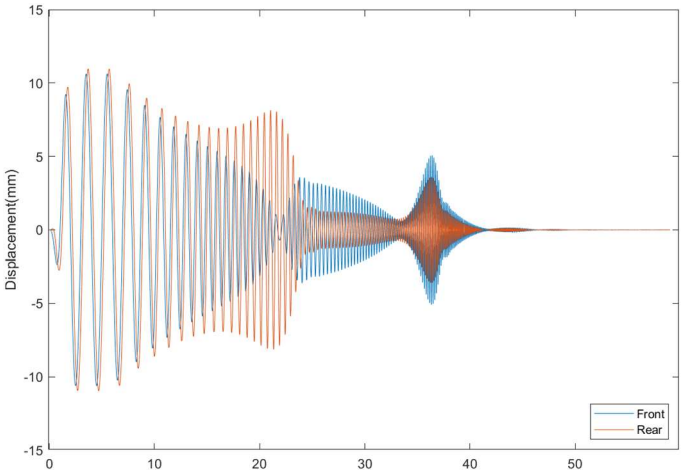

*Figure SEQ Figure * ARABIC 13. Front and Rear displacements when subject to the sweep motion.*

This factor, along with the offset centre of gravity, disturbs the displacement of the front and rear parts. It can be appreciated in Figure 13 that the rear is more subject to low frequency movements, while the front suffers a higher impact at higher frequencies, when compared to their pairs.

As being a linear damping model, only two parameters were studied: the front and rear damping ratios; against five different performance criteria: pitch, heave, front CPL variation, rear CPL variation and chassis acceleration.

The results for the optimal ratios along with the Cost Function Values and optimised ratios is shown in Table 6.

Optimisation Parameters	***Optimal damping ratios***		***Equivalent Damping Coefficients (newton-sec/mm)***		***COST FUNCTION VALUE***
	Front	*Rear*	*Front*	*Rear*	
Pitch	0.55	1.00	3.41	6.20	20.00%
Heave	0.10	0.10	0.62	0.62	5.00%
Front CPL	0.35	0.10	2.18	0.62	35.00%
Rear CPL	1.00	0.78	6.20	4.80	35.00%
Body Acceleration	0.77	1.00	4.77	6.20	5.00%
Cost Function	*0.42*	*0.90*	*2.60*	*5.58*	-

Table 6. Results for optimal damping ratios for the different optimisation parameters and their respective damping coefficient for the 4 degree of freedom model.

This model was produced as a starting point for further development, such as non-linear dampers, using the same method described above; and a further final upgrade to the 7 degrees of freedom model.

4 REFERENCES

Bäcker, M. (2016) 'CDTire: SCALABLE TIRE MODEL FOR FULL VEHICLE SIMULATIONS'. Available at: https://www.itwm.fraunhofer.de/content/dam/itwm/de/documents/MDF_Infomaterial/mdf_flyer_CD_Tire-EN.pdf

Dixon, J.C. (1996) *Tires, Suspension and Handling.* 2nd edn. London: Cambridge University Press.

Gallrein, A., Bäcker, M. (2007) 'CDTire: a tire model for comfort and durability applications', *Vehicle System Dynamics,* 45(1), pp 69-77. Available at: DOI: 10.1080/00423110801931771.

Gipser, M. '*FTire, a New Fast Tire Model for Ride Comfort Simulations'* . Available at: https://www.cosin.eu/wp-content/uploads/ftire_eng_1.pdf. (Accessed: 2 November 2022)

Gipser, M. (2007) 'FTire – the tire simulation model for all applications related to vehicle dynamics', *Vehicle System Dynamics*, 45:sup1, 139-151, DOI: 10.1080/00423110801899960

Mathworks (2022), *FTire and FTire/link.* Available at: https://www.mathworks.com/products/connections/product_detail/ftire.html. (Accessed: 29 October 2022)

Patel, M *et al*. (2015) 'A new multibody system approach for tire modeling using ANCF finite elements', *Proceedings of the Institution of Mechanical Engineers,* 230(1), pp. 69–84. Available at: DOI: 10.1177/1464419315574641

Shabana, A. (2015) 'ANCF reference node for multibody system analysis', *Journal of Multi-body Dynamics,* 229(1), pp. 109–112. Available at: DOI: 10.1177/1464419314546342

Suspension Secrets (n.d.) 'What is Slip Angle?', *Suspension Secrets*. Available at: https://suspensionsecrets.co.uk/tyre-slip-angle/ (Accessed: 12 December 2022)

Vogel, J. (n.d.) 'Tech Explained: Ackermann Steering Geometry', *Race Car Engineering*. Available at: https://www.racecar-engineering.com/articles/tech-explained-ackermann-steering-geometry/ (Accessed: 12 December 2022)